Inflated Kinetic Isotope Effects in the Branched Mechanism of *Neurospora crassa* 2-Nitropropane Dioxygenase†

Kevin Francis‡ and Giovanni Gadda*,§

Departments of Chemistry and Biology and The Center for Biotechnology and Drug Design, Georgia State University, Atlanta, Georgia 30302-4098

Received December 8, 2008; Revised Manuscript Received January 16, 2009

ABSTRACT: Catalytic turnover of *Neurospora crassa* 2-nitropropane dioxygenase with nitroethane as substrate occurs through both nonoxidative and oxidative pathways. The pH dependence of the kinetic isotope effects with [1,1-$^2H_2$]nitroethane as substrate was measured in the current study by monitoring the formation of the nitronate product in the nonoxidative pathway. The kinetic isotope effect on the second-order rate constant for nitronate formation, k_{cat}/K_m, decreased from an upper limiting value of 23 ± 1 at low pH to a lower limiting value of 11 ± 1 at high pH. These kinetic isotope effects are three times larger than those determined previously through measurements of oxygen consumption that occurs in the oxidative pathway of the enzyme [(2006) *Biochemistry 45*, 13889]. Analytical expressions for the k_{cat}/K_m values determined in each study show that the difference in the kinetic isotope effects arises from the branching of an enzyme−ethylnitronate reaction intermediate through oxidative and nonoxidative turnover. This branching is isotope sensitive due to a kinetic isotope effect on nitronate release rather than on flavin reduction as indicated by the pH-independent $^Dk_{red}$ value of 0.99 ± 0.06 with ethylnitronate as substrate. The kinetic isotope effect on ethylnitronate release arises from the deprotonation of histidine 196, which provides electrostatic interactions with the nitronate to keep it bound in the active site for oxidation. The isotope effect on branching results in an inflation of the kinetic isotope observed for the nonoxidative pathway to values that are larger than the intrinsic values associated with CH bond cleavage.

The use of kinetic isotope effects as mechanistic probes of enzymes with branched kinetic mechanisms is often complicated by isotope effects that are expressed on the partitioning of reaction intermediates formed during turnover. This has been best documented in the case of the cytochrome P450 class of enzymes (*1*−*3*) and the aromatic amino acid hydroxylases (*4*−*7*). The presence of branch points in a kinetic mechanism of an enzyme tends to reduce the observed kinetic isotope effect from the intrinsic values on bond cleavage as evident from the small kinetic isotope effects generally seen for these enzymes (*3, 8, 9*). The use of intramolecular isotope effects, to which extensive theory has been developed (*10*−*12*), has been successfully applied in the cytochrome P450 class of enzymes to unmask the effects of branching on the kinetic isotope effect for the reaction. In the case of the aromatic amino acid hydroxylases, the masking effects arising from branching have been overcome by uncoupling the reaction through site-directed mutagenesis (*13, 14*). This approach has been successfully employed with tyrosine hydroxylase (*13*) and recently with phenylalanine hydroxylase (*14*) to allow the intrinsic value for the kinetic isotope effect on CH bond cleavage to be observed in the reactions. In contrast to enzymatic reactions, branching of reaction intermediates to produce multiple products is a much more widely documented process for nonenzymatic reactions, where it has been demonstrated that it can result in an inflation or deflation of the observed kinetic isotope effects from the intrinsic value (*15*−*17*).

Recently, an FMN-dependent enzyme 2-nitropropane dioxygenase (2-NPD) from *Neurospora crassa* was demonstrated to utilize a branched catalytic cycle with either the neutral or anionic (nitronate) form of nitroethane as substrate (*18, 19*). The enzyme catalyzes the oxidative denitrification of nitroalkanes to the corresponding aldehyde compounds and nitrite through the formation of an anionic flavosemiquinone intermediate (*18*−*20*). As illustrated in Scheme 1, the branch point with nitroethane as substrate occurs after an isotope-sensitive step involving a proton abstraction reaction from the α-carbon of neutral nitroalkane catalyzed by histidine 196 (*19*). Branching occurs as a result of the partitioning of an enzyme−ethylnitronate transient intermediate formed with nitroethane as substrate through a nitronate dissociation step (k_{13} in Scheme 1) in a nonoxidative pathway and an electron transfer reaction with the flavin in an oxidative pathway (k_5 in Scheme 1). Reoxidation of the flavin in the oxidative pathway results in the formation of superoxide, which subsequently reacts with the enzyme-bound nitronate radical to form a peroxynitroethane inter-

† This work was supported in part by Grant PRF 47636-AC4 from the American Chemical Society (G.G.) and a Molecular Basis of Disease Fellowship from Georgia State University (K.F.). This work was presented at the Gordon Research Conference on Isotopes in Biological and Chemical Sciences in Ventura, CA, held Feb 17−22, 2008.

* Address correspondence to this author. Phone: (404) 413-5537. Fax: (404) 413-5505. E-mail: ggadda@gsu.edu.

‡ Department of Chemistry, Georgia State University.

§ Departments of Chemistry and Biology and The Center for Biotechnology and Drug Design, Georgia State University.

10.1021/bi802238j CCC: $40.75
Published on Web 02/06/2009

Scheme 1: Proposed Branch Point in the Steady-State Kinetic Mechanism of *N. crassa* 2-NPD with Nitroethane as Substrate[a]

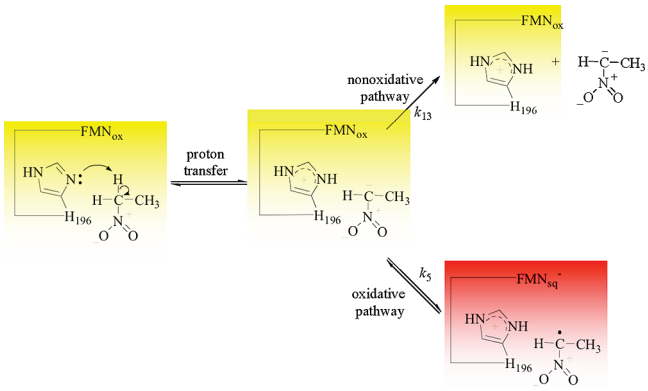

[a] The enzyme−ethylnitronate complex partitions through an oxidative catalytic pathway (via k_5) and a nonoxidative catalytic pathway (via k_{13}) at the branch point. Note that the kinetic step for the release of ethylnitronate (k_{13}) from the active site of the enzyme surface is shown as being irreversible because initial rates were measured in the absence of this species. For clarity, further kinetic steps occurring along the oxidative pathway are not shown.

mediate. This intermediate is then likely released from the active site, where it decays to give the acetaldehyde and nitrite products of the oxidative pathway. *N. crassa* 2-NPD can also utilize the deprotonated form of nitroethane as substrate, where a similar branching mechanism occurs as was demonstrated through measurements of the pH dependence of the secondary kinetic isotope effects with [1-^{2}H]ethylnitronate as substrate (*18*).

In the present study, the pH dependence of the kinetic isotope effects with nitroethane as substrate for the enzyme was determined by following the formation of the nitronate product formed during the nonoxidative pathway. The results were then compared with previous studies of the kinetic isotope effects with nitroethane as substrate measured by following oxygen consumption occurring during the oxidative pathway of the enzyme (*18*). The data indicate that the branching of reaction intermediates through multiple catalytic pathways results in an inflation of the observed kinetic isotope effects for the nonoxidative catalytic pathway as compared to that for nitroethane oxidation. This study represents the first instance in which an observed kinetic isotope effect in an enzymatic reaction is inflated above the intrinsic value associated with CH bond cleavage due to branch points occurring during catalytic turnover.

EXPERIMENTAL PROCEDURES

Materials. N. crassa 2-NPD was obtained using the expression and purification protocols described previously (*19*). Nitroethane and [1,1-^{2}H$_2$]nitroethane were from Sigma-Aldrich (St. Louis, MO). All other reagents were of the highest purity commercially available.

Methods. The kinetic parameters for the formation of ethylnitronate when nitroethane is used as substrate for *N. crassa* 2-NPD were determined by monitoring the increase in absorbance at 228 nm resulting from mixing the enzyme (1.07 μM final concentration) in air-saturated 50 mM sodium pyrophosphate with substrate (in the range from 1 to 3 mM final concentrations). The nonlinear time courses for the enzymatic reaction required the use of a logarithmic approach to determine initial rates, which was carried out as described previously (*19*). This approach was necessary to prevent an underestimation of the true initial rates for the reaction, which would result from arbitrarily considering only a portion of the reaction progress curve that might appear linear to the observer. Deuterium kinetic isotope effects were determined in assays carried out by alternating substrate isotopomers and were calculated from the ratio of the k_{cat}/K_m value obtained with unlabeled substrate to that with labeled substrate. The limited solubility of nitroethane prevented an accurate determination of the turnover numbers (k_{cat}), Michaelis constants (K_m), and the corresponding kinetic isotope effects for the enzyme with this substrate. The pH dependence of the $^D(k_{cat}/K_m)_{nox}$ values with [1,1-^{2}H$_2$]nitroethane as substrate was determined in air-saturated 50 mM sodium pyrophosphate in the pH range from 6.0 to 10.0 at 30 °C. Rates for the reductive half-reaction of the enzyme with ethylnitronate as substrate were determined at 30 °C using a TgK Scientific SF-61 stopped-flow spectrophotometer as previously described (*18*). The pH dependence of the reductive half-reaction was determined in the pH range from 6.0 to 10.1, by monitoring either the increase in absorbance at 370 nm (pH 7.0−10.1) or the decrease in absorbance at 444 nm (pH 6.0−6.5)[1] that results from the anaerobic mixing of the enzyme with the substrate. Nitronate solutions (100 mM) were prepared in water through incubation of the corresponding nitroalkane with a 1.2 M excess of potassium hydroxide for at least 24 h.

Data Analysis. Kinetic data were fit with KaleidaGraph software (Synergy Software, Reading, PA). For the nonenzymatic deprotonation of either nitroethane or [1,1-^{2}H$_2$]nitroethane, stopped-flow traces were fit with eq 1, which is a simplified expression for a pseudo-first-order reaction evaluated at initial rates (i.e., $t = 0$). A_0 is the initial absorbance at 228 nm, k_{obs} is the observed rate constant for the increase in absorbance at 228 nm, and t is time. The rate of product formation was determined from the k_{obs} value using the experimentally determined $\Delta\varepsilon_{228nm}$ value of 8520 M^{-1} cm^{-1}, which is the ε_{228nm} value for ethylnitronate corrected by the absorbance of nitroethane at that wavelength (*19*). Reaction progress curves with either nitroethane or [1,1-^{2}H$_2$]nitroethane as substrate for the enzyme were fit with eq 2, where A_0 is the initial absorbance at 228 nm, b is defined as a shape parameter, t is time, and x is the scale of the logarithmic curve. Initial rates were determined from the slope of a tangent line to the progress curve that intersects through the origin. This is found by taking the derivative of y in eq 2 with respect to t when the latter is set equal to zero (eq 3) and is converted to rates of nitronate formation using the experimentally determined $\Delta\varepsilon_{228nm}$ value[2] and correcting by the 1 cm path length (l) used as explained previously (*19*). The overall rate of product formation determined in

[1] The reductive half-reaction was monitored at 440 nm at pH values ≤6.5 because a species that absorbs light at 380 nm was observed upon mixing ethylnitronate with sodium pyrophosphate in the absence of enzyme (Francis and Gadda, unpublished observations). This species is likely a nitroethane dimer based on previous studies by Porter and Bright [(1977) *J. Biol. Chem. 252*, 4261−4370] but was not identified in this study because its formation is clearly nonenzymatic.

this fashion was converted to enzymatic reaction rates by subtraction of the nonenzymatic component determined under the same conditions. Second-order rate constants, $(k_{cat}/K_m)_{nox}$, for the enzymatic reaction of ethylnitronate formation and release were determined by fitting initial rate data to eq 4, where S is the concentration of substrate. The pH dependence of $(k_{cat}/K_m)_{nox}$ was determined by fitting the initial rate data to eq 5, which describes a curve with a slope of +1 and a plateau region at high pH. C is the pH-independent value of $(k_{cat}/K_m)_{nox}$ and K_a is the dissociation constant for the ionizable group. The pH dependence of both the $^D(k_{cat}/K_m)_{nox}$ value and the UV−visible absorbance spectrum of the enzyme was determined by fitting the data with eq 6, which describes a curve with plateau regions at both high and low pH. Y_L and Y_H are the limiting values at low and high pH, respectively, and K_a is the dissociation constant for the ionizable groups. Stopped-flow traces monitoring the reductive half-reaction of the enzyme were fit to eq 7, which describes a single exponential process where k_{obs} is the observed rate constant for flavin reduction, A_t is the absorbance at time t, and A is the final absorbance. Pre-steady-state kinetic parameters were determined using eq 8, where k_{obs} is the observed rate of flavin reduction, k_{red} is the limiting rate constant for flavin reduction at saturating substrate concentrations, K_d is the dissociation constant for substrate binding, and S is the concentration of substrate. The pH dependence of the reductive half-reaction was determined by fitting the data with eq 9, which describes a curve that decreases from an upper limiting value at low pH to a lower limiting plateau at an intermediate pH range and then with a slope of −1 at high pH. Y_L and Y_I are the limiting values at low and intermediate pH, respectively, and K_a is the dissociation constant for the ionizable groups.

$$v_0 = A_0 + k_{obs}t \tag{1}$$

$$A_{228} = A_0 + b\ln\left(1 + \frac{t}{x}\right) \tag{2}$$

$$v_0 = \left(\frac{b}{x}\right)\left(\frac{1}{\Delta\varepsilon_{228nm}l}\right) \tag{3}$$

$$\frac{v_0}{e} = \left(\frac{k_{cat}}{K_m}\right)_{nox} S \tag{4}$$

$$\log\left(\frac{k_{cat}}{K_m}\right)_{nox} = \log\left(\frac{C}{1 + \frac{10^{-pH}}{10^{-pK_a}}}\right) \tag{5}$$

$$\log Y = \log\frac{Y_L + Y_H\left(\frac{10^{-pK_a}}{10^{-pH}}\right)}{1 + \left(\frac{10^{-pK_a}}{10^{-pH}}\right)} \tag{6}$$

$$A_{total} = A_t e^{-k_{obs}t} + A \tag{7}$$

$$k_{obs} = \frac{k_{red}S}{K_d + S} \tag{8}$$

$$\log k_{red} = \log\left(\frac{Y_L}{1 + \frac{10^{-pK_{a_1}}}{10^{-pH}}} + \frac{Y_I}{1 + \frac{10^{-pK_{a_2}}}{10^{-pH}}}\right) \tag{9}$$

RESULTS

Effects of pH on the $^D(k_{cat}/K_m)_{nox}$ Values with Nitroethane as Substrate for the Nonoxidative Catalytic Pathway. The pH dependence of the kinetic isotope effect on the k_{cat}/K_m value of *N. crassa* 2-NPD with [1,1-$^2H_2$]nitroethane as substrate was determined in air-saturated 50 mM sodium pyrophosphate in the pH range from 6.0 to 10.0 at 30 °C by following nitronate formation during turnover. The kinetic isotope effect on the k_{cat}/K_m, denoted as $^D(k_{cat}/K_m)_{nox}$,[3] decreased from an upper limiting value of 23 ± 1 at low pH to a lower limiting value at high pH of 11 ± 1 (Figure 1A). For comparison, the pH profile of the $^D(k_{cat}/K_m)_{ox}$ values previously determined by measuring rates of oxygen consumption with [1,1-$^2H_2$]nitroethane as substrate yielded a similar pH-dependent behavior with limiting values of 7.4 ± 0.3 at low pH and 3.5 ± 0.1 at high pH (Figure 1A) (*18*). Those limiting values are 3.1 ± 0.2 and 3.1 ± 0.3 times lower than those determined here for $^D(k_{cat}/K_m)_{nox}$ at low and high pH, respectively. In agreement with previous studies on the pH profile of the $(k_{cat}/K_m)_{ox}$ values for the oxidative pathway (*19*), the pH profiles for the $(k_{cat}/K_m)_{nox}$ values with both nitroethane and [1,1-$^2H_2$]nitroethane as substrate showed the requirement for an unprotonated group for nitronate formation (Figure 1B). This is the expected pattern given that deprotonation of nitroethane occurs in a kinetic step that is common to both the nonoxidative and the oxidative catalytic pathways (Scheme 1). The kinetic parameters obtained by measuring nitronate formation and oxygen consumption are summarized in Table 1.

Effects of pH on the $^D(k_{red})$ Values with Ethylnitronate as Substrate for the Oxidative Catalytic Pathway. Previous studies have shown that the ethylnitronate product of the nonoxidative pathway of *N. crassa* 2-NPD is also an effective substrate for oxidative turnover of the enzyme (*18*−*20*). The pH dependence of the kinetic isotope effect on flavin reduction in the oxidative pathway of *N. crassa* 2-NPD with [1-^{2}H]ethylnitronate as substrate was determined in 50 mM sodium pyrophosphate in the pH range from 6.0 to 10.1 at 30 °C. Consistent with previous studies on the reductive half-

[2] The acetaldehyde and nitrite products of the oxidative pathway of the enzyme do not significantly absorb light at 228 nm as compared with ethylnitronate and were thus not taken into account when calculating rates of nitronate formation.

[3] For clarity, subscripts are placed next to the kinetic parameters described in this report to denote the method in which they were determined. Thus, $(k_{cat}/K_m)_{ox}$ refers to the kinetic parameter determined through measurements of oxygen consumption and $(k_{cat}/K_m)_{nox}$ refers to that obtained by following nitronate formation. The corresponding kinetic isotope effects on these values are expressed using the familiar superscript and are written as $^D(k_{cat}/K_m)_{ox}$ or $^D(k_{cat}/K_m)_{nox}$.

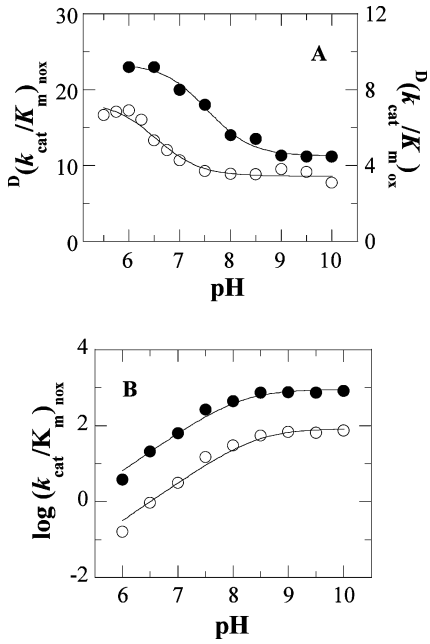

FIGURE 1: pH dependence of $^{D}(k_{cat}/K_m)_{nox}$ and $^{D}(k_{cat}/K_m)_{ox}$ with [1,1-^{2}H]nitroethane as substrate for *N. crassa* 2-NPD. Panel A: The $^{D}(k_{cat}/K_m)$ values were calculated from ratio of k_{cat}/K_m with nitroethane as substrate for the enzyme to that with [1,1-^{2}H]nitroethane measured by following nitronate formation (●) or oxygen consumption (○) during turnover. The data for $^{D}(k_{cat}/K_m)_{ox}$ are taken from ref *18*. Each curve is a fit of the data to eq 6. Panel B: The $(k_{cat}/K_m)_{nox}$ values were determined by monitoring the increase in absorbance at 228 nm that results from mixing enzyme with either nitroethane (●) or [1,1-^{2}H$_2$]nitroethane (○) as a function of pH at 30 °C. Data were fit with eq 5. The data for the $(k_{cat}/K_m)_{nox}$ pH profile are from ref *19*.

reaction of the enzyme (*18, 19*), anaerobic mixing of *N. crassa* 2-NPD with ethylnitronate resulted in the formation of an anionic flavosemiquinone with absorbance bands in the ~370 and ~470 nm regions (Figure 2A). As shown in Figure 2B for the example at pH 8.0, at any pH tested the rate of flavin reduction increased hyperbolically with substrate concentration and was the same irrespective of whether ethylnitronate or [1-^{2}H]ethylnitronate was used as substrate. Indeed, the kinetic isotope effect on the limiting rates of flavin reduction ($^{D}k_{red}$) was pH independent in the range from 6.0 to 10.1 with an average value of 0.99 ± 0.06 (Table 2). This is an expected result since the single electron transfer reaction from an enzyme-bound ethylnitronate to the flavin does not involve hybridization changes of the α-carbon of the substrate. The limiting rates of flavin reduction (k_{red}) with both isotopomers decreased from a limiting value of ~220 s^{-1} at low pH to lower values with increasing pH, showing the presence of two pK_a values for groups that need to be protonated for catalysis (Figure 2C). The lower pK_a values of 7.8 ± 0.1 and 8.0 ± 0.1 seen with ethylnitronate and [1-^{2}H]ethylnitronate, respectively, are consistent with previous results obtained on the steady-state kinetics for the oxidative pathway, suggesting the involvement of electrostatic catalysis in the formation of the anionic flavosemiquinone[4] (*18*). The requirement of a second protonated group with a pK_a value of ≥10.3 was also observed in the pH profiles of the k_{red} values (Figure 2C). This pK_a is possibly due to the deprotonation of the N(3) atom of the enzyme-bound FMN, which was independently shown in a pH titration of the UV−visible absorbance spectrum of the enzyme to have a pK_a of 10.9 ± 0.2 (Figure 3). The negative charge formed upon ionization of the N(3) atom of the flavin at high pH would prevent the single electron transfer reaction from the nitronate and would give rise to the pH dependence observed for the reductive half-reaction of the enzyme (Figure 2C).

DISCUSSION

Partitioning of reaction intermediates during turnover of an enzyme utilizing a branched kinetic mechanism can result in an inflation of the observed kinetic isotope effect well above the intrinsic value associated with bond cleavage as illustrated in the results of the current study. Branching during turnover of *N. crassa* 2-NPD with nitroethane as substrate occurs after the nitroalkane is deprotonated by histidine 196 (k_3) and involves the partitioning of the resulting enzyme−ethylnitronate complex through nonoxidative and oxidative pathways (Scheme 2) (*19*). Ethylnitronate is released as a reaction product during nonoxidative turnover (k_{13}), but is retained in the active site in the oxidative pathway that results from a single electron transfer reaction with the enzyme-bound flavin cofactor (k_5). The formation of the ethylnitronate product during nonoxidative turnover can be monitored spectrophotometrically to determine reaction rates as carried out in this and a previous study of the enzyme (*19*). Alternatively, rates of oxygen consumption during oxidative catalysis can be measured to determine enzymatic activity as described previously (*18*). Both methods have been used to measure the second-order rate constant, k_{cat}/K_m, for the reaction of *N. crassa* 2-NPD with nitroethane as substrate (*18, 19*). The k_{cat}/K_m values determined from these methods are fundamentally different kinetic parameters for the enzyme as evident from the differences in the magnitude, pH dependence, and extent to which a kinetic isotope effect is expressed when each assay is used to measure activity (*18, 19*).

The differences in the kinetic parameters determined by following either nitronate formation or oxygen consumption are readily explained by considering the branched nature of the catalytic cycle of the enzyme. The general definition of the k_{cat}/K_m value for an enzymatic reaction states that the kinetic parameter is a reflection of the rate of substrate capture into productive enzyme complexes destined to form products at some later time (*21, 22*). Branching during turnover of *N. crassa* 2-NPD with nitroethane as substrate results in multiple destinations for the enzyme−nitronate complex, which gives rise to the different k_{cat}/K_m values. Following the reaction by monitoring nitronate formation gives a $(k_{cat}/K_m)_{nox}$ value that reflects the rate of capture of nitroethane into productive complexes destined to form ethylnitronate at some later time (Scheme 2). When oxygen consumption is measured, the resulting $(k_{cat}/K_m)_{ox}$ value reflects capture rates for productive complexes destined to

[4] The pH profile of the k_{cat}/K_m value with ethylnitronate as substrate was previously fit to an equation describing the requirement of a single protonated group for catalysis [(2006) *Biochemistry 45*, 13889]. The fit resulted in an apparent outlier at pH 8.5 which, despite repeated measurements, showed a k_{cat}/K_m value lower than expected from the curve. The increased precision provided by the stopped-flow measurements reported here showed that the pH profile of the k_{red} value has a plateau region in the pH range from ~8.5 to 9.0. This plateau is likely displayed in the k_{cat}/K_m pH profile but was not defined due to the less precise measurements of enzyme activity reported in that study [(2006) *Biochemistry 45*, 13889].

Table 1: pH Dependence of the $(k_{cat}/K_m)_{nox}$ and $(k_{cat}/K_m)_{ox}$ Values of *N. crassa* 2-NPD with either Nitroethane or [1,1-^{2}H]Nitroethane as Substrate[a]

pH	$(k_{cat}/K_{NE})_{nox}$,[b,c] M^{-1} s^{-1}	$(k_{cat}/K_{DNE})_{nox}$,[d] M^{-1} s^{-1}	$(k_{cat}/K_{NE})_{ox}$,[b,e] M^{-1} s^{-1}	$(k_{cat}/K_{DNE})_{ox}$,[b,e] M^{-1} s^{-1}	$^D(k_{cat}/K_m)_{nox}$	$^D(k_{cat}/K_m)_{ox}$
6.0	4 ± 1	0.162 ± 0.004	50 ± 1	7 ± 1	23 ± 1	6.9 ± 0.1
6.5	20 ± 1	0.925 ± 0.045	100 ± 4	20 ± 1	23 ± 1	5.0 ± 0.3
7.0	60 ± 2	3.11 ± 0.05	200 ± 10	50 ± 2	20 ± 1	4.3 ± 0.1
7.5	265 ± 4	14.7 ± 0.2	350 ± 5	95 ± 5	18 ± 1	3.7 ± 0.2
8.0	450 ± 10	30 ± 2	675 ± 20	180 ± 5	14 ± 1	3.6 ± 0.2
8.5	730 ± 16	54 ± 2	800 ± 25	225 ± 15	13 ± 1	3.6 ± 0.1
9.0	760 ± 10	68 ± 1	375 ± 20	100 ± 10	11 ± 1	3.7 ± 0.4
9.5	740 ± 23	66 ± 3	185 ± 10	50 ± 3	11 ± 1	3.7 ± 0.3
10.0	830 ± 25	74 ± 3	155 ± 10	50 ± 4	11 ± 1	3.1 ± 0.3

[a] All assays were carried out in 50 mM sodium pyrophosphate at 30 °C. [b] With nitroethane as substrate. [c] From ref *19*. [d] With [1,1-^{2}H]nitroethane as substrate. [e] From ref *18*.

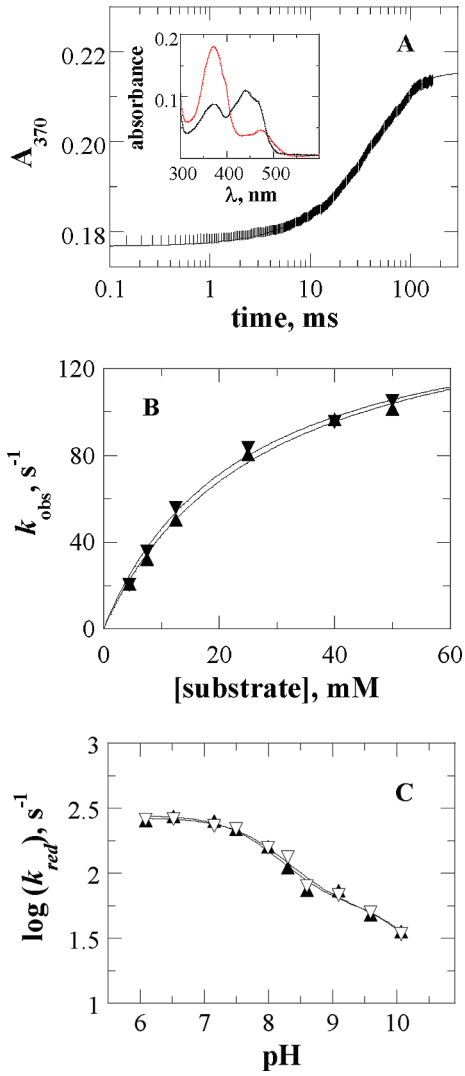

FIGURE 2: pH dependence of the $^Dk_{red}$ value with [1-^{2}H]ethylnitronate as substrate for *N. crassa* 2-NPD. Panel A: The absorbance at 370 nm was monitored over time after anaerobic mixing of *N. crassa* 2-NPD with ethylnitronate at pH 8.0 and 30 °C to give final concentrations of 15 μM enzyme and 4.5 mM substrate. The time indicated is after the end of flow (2.2 ms). Inset: Flavin absorbance spectra before (black) and ~30 s after (red) anaerobic mixing of the enzyme with ethylnitronate. Panel B: Rates of flavin reduction determined from fits of stopped-flow traces to eq 7 were plotted as a function of either ethylnitronate (▲) or [1-^{2}H]ethylnitronate (▼) concentration and were fit with eq 8 to obtain limiting rates of flavin reduction (k_{red}). Panel C: The pH profile of k_{red} with ethylnitronate (▲) or [1-^{2}H]ethylnitronate (▽) in the pH range from 6.0 to 10.1. The data were fit with eq 9.

form the products of the oxidative catalytic pathway of the enzyme (Scheme 2).

Branching of the enzyme−ethylnitronate intermediate formed with nitroethane as substrate for *N. crassa* 2-NPD affects the k_{cat}/K_m values for the reaction because all of the kinetic steps leading to its formation are reversible (Scheme 2). In general, an analytical expression for the k_{cat}/K_m value of an enzymatic reaction includes rate constants for all kinetic steps from substrate binding up to and including the first irreversible step of the mechanism (*23*). As shown in Scheme 2, the branch point in the kinetic mechanism of *N. crassa* 2-NPD occurs after the reversible steps of substrate binding (k_1, k_2) and the proton abstraction with histidine 196 (k_3, k_4). Substrate binding is reversible at the low concentrations of nitroethane used when k_{cat}/K_m is measured. The subsequent proton transfer reaction is also reversible as evident from previous studies demonstrating that the enzyme utilizes a sequential steady-state kinetic mechanism with nitroethane as substrate (*18, 20*). The reversibility of the steps leading to the branch point expands the expression for k_{cat}/K_m to include all of the rate constants leading to the first irreversible steps of each catalytic pathway of the enzyme. In the nonoxidative pathway this includes only the nitronate release step (k_{13}), which is irreversible because initial rates were measured in the absence of ethylnitronate. At large concentrations of oxygen, the net flux of the enzyme−nitronate intermediate through the flavin reduction step (k_5, k_6) in the oxidative pathway becomes practically irreversible (*23*). This stems from the bimolecular oxidation of the flavosemiquinone becoming significantly faster than its formation (i.e., $O_2k_7 \gg k_5$) when oxygen concentration is large, thereby depleting the steady-state concentration of the reduced enzyme−nitronate radical complex (E_{sq}−S$^\bullet$ in Scheme 2) that would be needed for the reverse electron transfer reaction (k_6). The k_{cat}/K_m values for the *N. crassa* 2-NPD reaction therefore include only the kinetic steps for the formation and breakdown of the enzyme−nitroethane Michaelis complex (k_1, k_2), the reversible proton abstraction from the nitroalkane (k_3, k_4), and the partitioning of the enzyme−nitronate complex through the release of ethylnitronate as a product (k_{13}) and flavin reduction (k_5). Expressions for both $(k_{cat}/K_m)_{nox}$ and $(k_{cat}/K_m)_{ox}$ were derived using the method of King and Altman (*24*) to give eqs 10 and 11:[5]

$$\left(\frac{k_{cat}}{K_m}\right)_{nox} = k_{13}\left(\frac{k_1k_3}{k_2(k_4 + k_5 + k_{13})}\right) \quad (10)$$

$$\left(\frac{k_{cat}}{K_m}\right)_{ox} = k_5\left(\frac{k_1k_3}{k_2(k_4 + k_5 + k_{13})}\right) \quad (11)$$

A comparison of the k_{cat}/K_m values with nitroethane as substrate for *N. crassa* 2-NPD reveals how the enzyme−ethyl-

Table 2: pH Dependence of the Reductive Half-Reaction of *N. crassa* 2-NPD with either Ethylnitronate or [1-^{2}H]Ethylnitronate as Substrate[a]

pH	$k_{red(H)}$,[b] s^{-1}	$k_{red(D)}$,[c] s^{-1}	$^Dk_{red}$	$K_{d(H)}$,[b] mM	$K_{d(D)}$,[c] mM
6.1	255 ± 30	260 ± 70	1.0 ± 0.3	15 ± 2	15 ± 5
6.5	270 ± 90	260 ± 90	1.0 ± 0.5	25 ± 10	30 ± 10
7.15	250 ± 10	230 ± 10	1.1 ± 0.1	30 ± 3	25 ± 2
7.5	220 ± 10	220 ± 10	1.1 ± 0.1	25 ± 2	30 ± 3
8.0	160 ± 10	160 ± 10	1.1 ± 0.1	30 ± 3	25 ± 4
8.3	110 ± 3	125 ± 5	0.9 ± 0.1	10 ± 1	10 ± 1
8.6	75 ± 10	80 ± 10	0.9 ± 0.1	35 ± 6	40 ± 7
9.1	70 ± 5	70 ± 5	1.0 ± 0.1	25 ± 5	20 ± 3
9.6	50 ± 4	50 ± 5	1.0 ± 0.1	40 ± 5	40 ± 10
10.1	35 ± 2	35 ± 3	1.0 ± 0.1	20 ± 5	20 ± 5

[a] *N. crassa* 2-NPD was anaerobically mixed with substrate in 50 mM sodium pyrophosphate at 30 °C in a stopped-flow spectrophotometer, and the absorbance changes at 370 or 440 nm were monitored over time. [b] With ethylnitronate as substrate. [c] With [1-^{2}H]ethylnitronate as substrate.

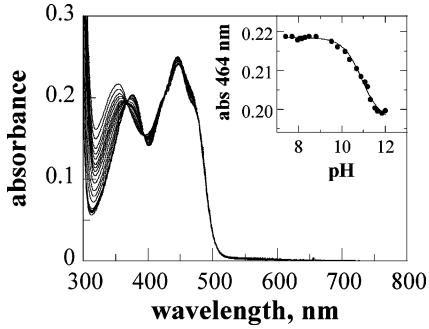

FIGURE 3: pH dependence of the UV−visible absorbance properties of *N. crassa* 2-NPD. UV−visible absorbance spectra of the enzyme (21 μM) were recorded in 50 mM sodium phosphate at 10 °C in the pH range from 7.4 to 12.0. Inset: UV−visible absorbance values at 464 nm as a function of pH. The data were fit with eq 6.

Scheme 2: Proposed Steady-State Kinetic Mechanism of *N. crassa* 2-NPD with Nitroethane as Substrate[a]

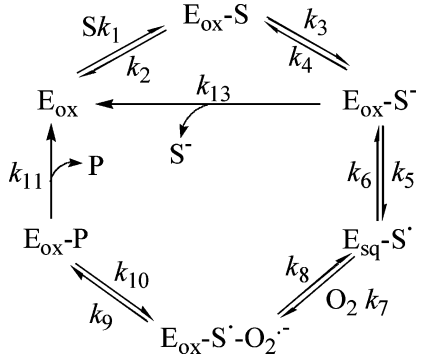

[a] E_{ox} is the oxidized form of enzyme; E_{sq} is the flavosemiquinone form of enzyme; S is nitroethane; S^- is ethylnitronate; $S^\bullet$ and P are a radical intermediate and the product of the oxidative pathway of the enzyme, respectively. Note that the kinetic steps for the release of ethylnitronate (S^-) and the oxidative product (P) are shown as being irreversible because initial rates were measured in the absence of these species.

nitronate complex formed during turnover partitions through the nonoxidative and oxidative catalytic pathways. Each value describes identical productive complexes that form as a result of nitroethane binding to the enzyme (k_1) and the deprotonation of the nitroalkane by the active site residue histidine 196 (k_3) (*19*). Since the same productive complexes are described by each expression, the kinetic steps leading to their steady-state formation and breakdown must also be the same. This is reflected in the parentheses of the expressions for k_{cat}/K_m shown in eqs 10 and 11. Taking the ratio of these k_{cat}/K_m values cancels the terms in the parentheses to provide a direct measure of how the enzyme−ethylnitronate complex partitions between nitronate release (k_{13}) and flavin reduction (k_5) as shown in eq 12. The partition ratios (P) of the *N. crassa* 2-NPD reaction with either nitroethane or [1,1-^{2}H]nitroethane calculated from eq 12 are shown in Table 3.

Table 3: Partition Ratios with Nitroethane or [1,1-^{2}H]Nitroethane as Substrate for *N. crassa* 2-NPD[a]

pH	P_H[b]	P_D[b]	P_H/P_D
6.0	0.08 ± 0.02	0.023 ± 0.003	3.5 ± 1.0
6.5	0.20 ± 0.01	0.046 ± 0.003	4.3 ± 0.4
7.0	0.30 ± 0.02	0.062 ± 0.003	4.8 ± 0.4
7.5	0.76 ± 0.02	0.16 ± 0.01	4.8 ± 0.3
8.0	0.67 ± 0.03	0.17 ± 0.01	3.9 ± 0.3
8.5	0.91 ± 0.04	0.24 ± 0.02	3.8 ± 0.3
9.0	2.0 ± 0.1	0.68 ± 0.07	2.9 ± 0.3
9.5	4.0 ± 0.3	1.3 ± 0.1	3.1 ± 0.3
10.0	5.4 ± 0.4	1.5 ± 0.1	3.6 ± 0.4

[a] In 50 mM sodium pyrophosphate at 30 °C. [b] Partition ratios with nitroethane (P_H) or [1,1-^{2}H]nitroethane (P_D) were obtained by dividing the k_{cat}/K_m value measured by monitoring rates of nitronate formation to that determined by measuring rates of oxygen consumption.

$$P = \frac{(k_{cat}/K_m)_{nox}}{(k_{cat}/K_m)_{ox}} = \frac{k_{13}}{k_5} \quad (12)$$

A partition isotope effect is expressed on the *N. crassa* 2-NPD reaction as the result of a kinetic isotope effect on the release of the nitronate formed with either nitroethane or [1,1-^{2}H]nitroethane as substrate. Evidence supporting this conclusion comes from the differences in the partition ratios calculated with nitroethane and [1,1-^{2}H]nitroethane (Table 3) and the lack of a kinetic isotope effect on the reductive half-reaction of the enzyme. Partition ratios for the reaction catalyzed by *N. crassa* 2-NPD reflect the relative rates of nitronate release (k_{13}) and flavin reduction (k_5) (eq 12). Since the limiting rate constant for flavin reduction with ethylni-

[5] The simplified expressions for k_{cat}/K_m are based on experimental data made in a previous report [(2006) *Biochemistry 45*, 13889] showing that the enzyme is saturated with oxygen under atmospheric conditions across the pH range tested and that the kinetic step $k_2 \gg k_3$. This was shown through measurements of the K_m for oxygen and from the lack of solvent viscosity effects on the $(k_{cat}/K_m)_{ox}$ value with nitroethane as substrate for the enzyme, respectively. The previous derivation of $(k_{cat}/K_m)_{ox}$ assumed that $k_{13} \gg k_5$ based on the lack of solvent viscosity effects on k_{cat}/K_m with ethylnitronate as substrate [(2006) *Biochemistry 45*, 13889]. This assumption was not applied in the current study with nitroethane as substrate because the observation of both oxygen consumption and nitronate release during turnover clearly demonstrates that k_{13} is comparable to k_5.

tronate is not isotope sensitive, the partition isotope effect must arise from different rates of nitronate release with nitroethane or [1,1-^{2}H]nitroethane as substrate for the enzyme. The kinetic isotope effect on nitronate release likely arises from the deprotonation of histidine 196, which was previously shown to be the catalytic base for the reaction of the enzyme with nitroethane as substrate (*19*). The positive charge formed on the imidazolium side chain of histidine 196 as a result of the proton transfer reaction with nitroethane likely establishes electrostatic interactions with the anionic nitronate intermediate to keep it bound in the active site for oxidation. Deprotonation of histidine 196 would disrupt these interactions to promote nitronate release and would be isotope sensitive since it involves the transfer of a deuteron instead of a proton when [1,1-^{2}H]nitroethane is the substrate. The role of histidine 196 for nitronate release is supported by both the partition ratios for the reaction, which increase with increasing pH, and the magnitude of the partition isotope effects of the reaction (Table 3), which is within the range from 3 to 4 that was previously reported for the kinetic isotope effect on the deprotonation of imidazolium (*25, 26*).

The partition isotope effect expressed on nonoxidative turnover of *N. crassa* 2-NPD with nitroethane as substrate inflates the observed limiting $^{D}(k_{cat}/K_m)_{nox}$ above the intrinsic value associated with the deprotonation of the nitroalkane. The increase in the limiting value of the $^{D}(k_{cat}/K_m)_{nox}$ at low pH from that previously determined for $^{D}(k_{cat}/K_m)_{ox}$ (i.e., 23 versus 7.4 at low pH) (*18*) corresponds well with the partition isotope effect of ~3 that can be calculated from the P_H and P_D values shown in Table 3. Only the limiting values of $^{D}(k_{cat}/K_m)$ can be compared in this analysis because pH effects alter the kinetic isotope effects measured with each assay (eqs 13 and 14; derivations are shown in the Supporting Information). As the pH is raised above the pK_a of histidine 196, the rate constant for nitronate release (k_{13}) increases, while the rate constants for nitronate oxidation (k_5) and protonation (k_4) decrease to a limiting value and zero, respectively. Thus, the partition ratio increases from a lower limiting value at low pH to an upper limiting value at high pH, while the reverse commitment to catalysis decreases from an upper limiting value at low pH to zero. As shown in eqs 13 and 14, the increase in the partition ratio with increasing pH results in a decrease in the $^{D}(k_{cat}/K_m)$ values for the reaction. Since the isotope effect on the partition ratio arises from different rates of nitronate release (k_{13}) during nonoxidative turnover of the enzyme with nitroethane as substrate and not from different rates of electron transfer (k_5), it is only expressed on $^{D}(k_{cat}/K_m)_{nox}$ (eq 14). As shown in eq 14, the overall $^{D}(k_{cat}/K_m)_{nox}$ value of *N. crassa* 2-NPD is therefore given by both a primary isotope effect arising from CH bond cleavage ($^{D}(k_{cat}/K_m)_{ox}$) and a partition isotope effect resulting from different rates of nitronate release with nitroethane and [1,1-^{2}H]nitroethane as substrate ($^{D}k_{13}$). Thus, the limiting $^{D}(k_{cat}/K_m)_{nox}$ of ~23 is inflated from the intrinsic value ~8−9, which was previously measured for the deprotonation of nitroethane in solution (*27, 28*).

$$^{D}\left(\frac{k_{cat}}{K_m}\right)_{ox} = \frac{^{D}k_3 + {}^{D}k_3\left(\frac{1}{^{D}k_{13}}P\right) + {}^{D}K_{eq3}C_r}{1 + C_r + P} \qquad (13)$$

where $P = k_{13}/k_5$, $C_r = k_4/k_5$, and $^{D}K_{eq3} = {}^{D}k_3/{}^{D}k_4$.

$$^{D}\left(\frac{k_{cat}}{K_m}\right)_{nox} = {}^{D}k_{13}\,{}^{D}\left(\frac{k_{cat}}{K_m}\right)_{ox} \qquad (14)$$

The present investigation of the *N. crassa* 2-NPD reaction represents the first instance of an enzymatic reaction where the observed kinetic isotope effect is inflated well above the intrinsic value that is associated with CH bond cleavage because of the branching of a reaction intermediate. This study therefore complements previous works on other enzymes showing that branching of reaction intermediates can inflate observed kinetic isotope effects observed for one pathway to their intrinsic values (*7, 13*) or, as is more commonly observed, decrease the magnitude of the observed kinetic isotope effect (*1*−*5, 29*). A rate-limiting step involving bond cleavage may therefore give rise to a kinetic isotope effect that is inflated from the intrinsic value or is completely abated due to the presence of branching in the kinetic mechanism of an enzyme.

ACKNOWLEDGMENT

The authors are indebted to all of their colleagues for insightful suggestions. In particular, we extend our appreciation to Drs. Phil Huskey, Charles Perrin, John Groves, Bruce Palfey, and John Richard. We also thank Ms. Hongling Yuan for the determination of the pH dependence of the UV−visible absorbance spectrum of the enzyme and all of the colleagues who reviewed this study, whose thoughtful criticisms and insights resulted in a significant improvement of the manuscript.

SUPPORTING INFORMATION AVAILABLE

The mathematic derivations of eqs 10, 11, 13, and 14 illustrating the k_{cat}/K_m values for nitroethane as substrate for the nonoxidative and oxidative pathways and the corresponding kinetic isotope effects catalyzed by the enzyme. This material is available free of charge via the Internet at http://pubs.acs.org.

REFERENCES

1. Austin, R. N., Deng, D., Jiang, Y., Luddy, K., van Beilen, J. B., Ortiz de Montellano, P. R., and Groves, J. T. (2006) The diagnostic substrate bicyclohexane reveals a radical mechanism for bacterial cytochrome P450 in whole cells. *Angew. Chem., Int. Ed. Engl. 45*, 8192–8194.
2. Jiang, Y., He, X., and Ortiz de Montellano, P. R. (2006) Radical intermediates in the catalytic oxidation of hydrocarbons by bacterial and human cytochrome P450 enzymes. *Biochemistry 45*, 533–542.
3. Guengerich, F. P., Miller, G. P., Hanna, I. H., Sato, H., and Martin, M. V. (2002) Oxidation of methoxyphenethylamines by cytochrome P450 2D6. Analysis of rate-limiting steps. *J. Biol. Chem. 277*, 33711–33719.
4. Pavon, J. A., and Fitzpatrick, P. F. (2005) Intrinsic isotope effects on benzylic hydroxylation by the aromatic amino acid hydroxylases: evidence for hydrogen tunneling, coupled motion, and similar reactivities. *J. Am. Chem. Soc. 127*, 16414–16415.
5. Hillas, P. J., and Fitzpatrick, P. F. (1996) A mechanism for hydroxylation by tyrosine hydroxylase based on partitioning of substituted phenylalanines. *Biochemistry 35*, 6969–6975.
6. Fitzpatrick, P. F. (2003) Mechanism of aromatic amino acid hydroxylation. *Biochemistry 42*, 14083–14091.
7. Fitzpatrick, P. F. (2006) Isotope Effects from Partitioning of Intermediates in Enzyme-Catalyzed Hydroxylation Reactions, in *Isotope Effects in Chemistry and Biology* (Kohen, A., and Limbach, H. H., Eds.) pp 861−873, Taylor and Francis, Boca Raton, FL.
8. Korzekwa, K. R., Swinney, D. C., and Trager, W. F. (1989) Isotopically labeled chlorobenzenes as probes for the mechanism

of cytochrome P-450 catalyzed aromatic hydroxylation. *Biochemistry 28*, 9019–9027.

9. Higgins, L., Bennett, G. A., Shimoji, M., and Jones, J. P. (1998) Evaluation of cytochrome P450 mechanism and kinetics using kinetic deuterium isotope effects. *Biochemistry 37*, 7039–7046.
10. Miwa, G. T., Garland, W. A., Hodshon, B. J., Lu, A. Y., and Northrop, D. B. (1980) Kinetic isotope effects in cytochrome P-450-catalyzed oxidation reactions. Intermolecular and intramolecular deuterium isotope effects during the N-demethylation of N,N-dimethylphentermine. *J. Biol. Chem. 255*, 6049–6054.
11. Jones, J. P., Korzekwa, K. R., Rettie, A. E., and Trager, W. F. (1986) Isotopically sensitive branching and its effect on the observed intramolecular isotope effects in cytochrome P-450 catalyzed reactions: a new method for the estimation of intrinsic isotope effects. *J. Am. Chem. Soc. 108*, 7074–7078.
12. Korzekwa, K. R., Trager, W. F., and Gillette, J. R. (1989) Theory for the observed isotope effects from enzymatic systems that form multiple products via branched reaction pathways: cytochrome P-450. *Biochemistry 28*, 9012–9018.
13. Frantom, P. A., and Fitzpatrick, P. F. (2003) Uncoupled forms of tyrosine hydroxylase unmask kinetic isotope effects on chemical steps. *J. Am. Chem. Soc. 125*, 16190–16191.
14. Panay, A. J., and Fitzpatrick, P. F. (2008) Kinetic isotope effects on aromatic and benzylic hydroxylation by *Chromobacterium violaceum* phenylalanine hydroxylase as probes of chemical mechanism and reactivity. *Biochemistry 47*, 11118–111124.
15. Thibblin, A. (1989) Reaction branching and extreme kinetic isotope effects in the study of reaction mechanisms. *Chem. Soc. Rev. 18*, 209–224.
16. Thibblin, A. (1988) Reaction branching as a mechanistic alternative to tunneling in explaining anomalous temperature dependencies of kinetic isotope effects. *J. Phys. Org. Chem. 1*, 161–167.
17. Oelwegaard, M., McEwen, I., Thibblin, A., and Ahlberg, P. (1985) Stepwise base-promoted elimination of hydrochloric acid via hydrogen-bonded carbanions studied by reaction branching and extreme deuterium isotope effects. Parallel carbocationic and carbanionic reactions. *J. Am. Chem. Soc. 107*, 7494–7499.
18. Francis, K., and Gadda, G. (2006) Probing the chemical steps of nitroalkane oxidation catalyzed by 2-nitropropane dioxygenase with solvent viscosity, pH, and substrate kinetic isotope effects. *Biochemistry 45*, 13889–13898.
19. Francis, K., and Gadda, G. (2008) The nonoxidative conversion of nitroethane to ethylnitronate in *Neurospora crassa* 2-nitropropane dioxygenase is catalyzed by His-196. *Biochemistry 47*, 9136–9144.
20. Francis, K., Russell, B., and Gadda, G. (2005) Involvement of a flavosemiquinone in the enzymatic oxidation of nitroalkanes catalyzed by 2-nitropropane dioxygenase. *J. Biol. Chem. 280*, 5195–5204.
21. Northrop, D. B. (1998) On the meaning of K_m and V/K in enzyme kinetics. *J. Chem. Educ. 75*, 1153–1157.
22. Northrop, D. B. (1999) So what exactly is V/K, anyway? *Biomed. Health Res. 27*, 250–263.
23. Cleland, W. W. (1975) Partition analysis and the concept of net rate constants as tools in enzyme kinetics. *Biochemistry 14*, 3220–3224.
24. King, E. L., and Altman, C. (1956) A schematic method of deriving the rate laws for enzyme-catalyzed reactions. *J. Phys. Chem. 60*, 1375–1378.
25. Jencks, W. P., and Carriuolo, J. (1959) Imidazole catalysis. III. General base catalysis and the reactions of acetyl imidazole with thiols and amines. *J. Biol. Chem. 234*, 1280–1285.
26. Jencks, W. P., and Carriuolo, J. (1961) General base catalysis of ester hydrolysis. *J. Am. Chem. Soc. 83*, 1743–1749.
27. Gadda, G., Choe, D. Y., and Fitzpatrick, P. F. (2000) Use of pH and kinetic isotope effects to dissect the effects of substrate size on binding and catalysis by nitroalkane oxidase. *Arch. Biochem. Biophys. 382*, 138–144.
28. Valley, M. P., and Fitzpatrick, P. F. (2004) Comparison of enzymatic and non-enzymatic nitroethane anion formation: thermodynamics and contribution of tunneling. *J. Am. Chem. Soc. 126*, 6244–6245.
29. Guengerich, F. P. (1991) Reactions and significance of cytochrome P-450 enzymes. *J. Biol. Chem. 266*, 10019–10022.

BI802238J